NSRRC-J04994 (2015)

THE JOURNAL OF CHEMICAL PHYSICS 142, 184903 (2015)

The dispersion state of magnetic nanorods in homopolymers and block copolymers

Chieh-Tsung Lo,[a] Ming-Hsuan Li,[b] and Wei-Ting Lin[b]
Department of Chemical Engineering, National Cheng Kung University, No. 1, University Road, Tainan City 701, Taiwan

(Received 23 March 2015; accepted 30 April 2015; published online 13 May 2015)

We investigated the dispersion state of pyridine-modified magnetic nanorods in poly(2 vinylpyridine) (P2VP) homopolymers and poly(styrene-b-2 vinylpyridine) (PS-P2VP) diblock copolymers. In the P2VP/nanorod mixtures, the dispersion of nanorods was enhanced in systems in which the molecular weight of P2VP was increased because the long P2VP chains provided steric hindrance and thus screened the attractive interparticle interactions, inhibiting the rod aggregation. When nanorods were mixed with PS-P2VP, the phase stability of the mixtures varied considerably according to changes in the lamellar period of PS-P2VP (D). When D was large, nanorods were sequestered into the P2VP domains through enthalpically driven self-assembly, and the nanorods became spatially organized. By contrast, when D was small, the introduction of nanorods caused substantial distortion of chain conformations. This entropically unfavorable condition can be offset by excluding nanorods from the ordered phases, causing particle aggregation. At a high particle loading, the attractive interparticle interactions outweighed the particle–polymer interaction and entropic contribution of polymers. Consequently, nanorods underwent extensive aggregation. © *2015 AIP Publishing LLC.* [http://dx.doi.org/10.1063/1.4921042]

INTRODUCTION

Magnetic nanoparticles exhibit valuable fundamental properties and have become central constituents of various nanotechnological applications, such as data storage media,[1,2] spin-dependent electron transport devices,[3] therapeutic and diagnostic medical devices,[4,5] and environmental remediation systems.[6,7] To develop magnetic nanomaterials, the manipulation of nanoparticles in a designable media is crucial because it enables the functional properties of the materials to be controlled. For example, magnetic nanoparticles can be incorporated into a dielectric or nonmagnetic metal matrix to obtain magneto-resistive properties.[8,9] Moreover, magnetic nanoparticles can be incorporated into biomaterials to enable magnetic field-assisted drug delivery.[10,11]

The control of particle dispersion and the assembly of particles into a functional nanostructure are crucial to the development of nanoparticles that satisfy the requirements for commercial application.[12–14] For example, self assembly of spherical nanoparticles into anisotropic structures in a polymer matrix facilitated the solid-like reinforcement of the mechanical properties of the polymer.[15,16] Du suggested that dispersing anisotropic particles in a polymer matrix changed the linear viscoelastic properties of the composites from liquid-like to solid-like characteristics because of the formation of percolated filler networks.[17] These percolating networks can potentially improve the mechanical properties of the nanocomposites,[18] and rods and platelets offer favorable reinforcement over spheres.[19] The control of particle dispersion is a formidable challenge for magnetic nanoparticles because the magnetic dipole–dipole interaction between particles can cause particle aggregation. Several studies have reported using polymers as building blocks to design magnetic nanomaterials and have addressed comprehensively the physics involved in organizing magnetic nanoparticles in polymer matrices.[20–26] Combining these two physically different constituents yields products that feature the cooperative performance of magnetic nanoparticles and the processability of polymers. Like the dispersion of noninteracting particles in polymers, the dispersion of magnetic nanoparticles in polymers can be enhanced effectively by grafting ligands on the particle surface, and the phase behavior of the mixtures depends strongly on the ratio between the mass of the grafted chains and that of the polymer matrix.[23] When the ratio was lower than 1, ramified aggregates developed. The particle aggregates were oriented further by applying a magnetic field. By contrast, particles were dispersed uniformly when the mass of the grafted chains and that of the polymer matrix were identical. Jiao and Akcora suggested that brush–brush entanglement on polymer-grafted iron oxide nanoparticles played an effective role in forming a particle string.[24] When anisotropic particles were introduced, magnetic dipole–dipole interaction caused the particles to aggregate in structures ranging from loosely packed clusters to antiparallel packed clusters as particle loading was increased.[25] Studies on polymer/magnetic nanoparticle composites have mainly sought to obtain either a perfect dispersion of particles or a percolated network of aggregated particles.

[a]Author to whom correspondence should be addressed. Electronic mail: tsunglo@mail.ncku.edu.tw, Tel.: +886-6-2757575 ext. 62647. Fax: +886-6-2344496.
[b]Electronic addresses: hank_aqu076@hotmail.com and weiting323@gmail.com

 ©2015 AIP Publishing LLC

This article is copyrighted as indicated in the article. Reuse of AIP content is subject to the terms at: http://scitation.aip.org/termsconditions. Downloaded to IP: 140.110.200.41 On: Thu, 31 Dec 2015 02:28:59

A recently developed approach for manipulating the spatial distribution of magnetic nanoparticles is to use block copolymers as a scaffold. Block copolymers consist of chemically different constituents that are covalently bonded to form a single polymer chain. Because the two chemical species are energetically unfavorable, the respective blocks tend to microphase separate, forming a rich diversity of structures at nanometer-length scales.[27] These ordered structures can serve as an effective platform on which to control particle location and dispersion. However, introducing nanoparticles to block copolymers creates additional complexities because multiple interactions occur between various constituents and confinement effects. Considerable progress has been achieved experimentally in assembling magnetic nanoparticles selectively into the distinct microdomains of block copolymers to create two-dimensional and three-dimensional spatial distributions of nanoparticles.[28–42] For example, Sohn and Cohen prepared free-standing block copolymer films containing γ-Fe_2O_3 nanoparticles by using static casting.[28] The particles were dispersed uniformly within interconnected cylindrical microdomains and exhibited superparamagnetic behavior. Hamdoun investigated the effect of the particle size on the dispersion γ-Fe_2O_3 nanoparticles in lamellar-ordered block copolymers.[30,31] Dispersing large particles caused chain stretching, causing particles to segregate from the ordered phase of block copolymers. A homopolymer can be introduced into the system to compensate for the phase deformation, thus enabling the particle loading to be increased without disturbing the polymer morphology. By contrast, although dispersing small particles also caused chain stretching, the increase in the translational entropy of particles induced by particle dispersion compensated for the loss of the conformational entropy of the polymer. Xu *et al.* suggested controlling particle dispersion by manipulating the relative molecular weight of the grafted polymer brushes and block copolymers.[37,38] When magnetic nanoparticles were grafted with long brushes, the particles aggregated and ordered phases assembled around the aggregates to form onion-ring-like features. By contrast, the nanoparticles dispersed uniformly in the preferred domains of the block copolymer when they were grafted with short brushes. The phase behavior of block copolymer/magnetic nanoparticle mixtures also varies according to the casting solvent used.[35,39] When a good solvent for both blocks was used, magnetic nanoparticles aggregated during solvent evaporation. The aggregated particles could trigger a morphological transition of block copolymers from hexagonally packed cylinders to undulated cylinders to body-centered cubic spheres. By contrast, in a mixture of a block copolymer and magnetic nanoparticles cast with a selective solvent, the nanoparticles were trapped into the preferred domains through the facile inversion of micelles during solvent evaporation. Consequently, the block copolymer lost its long-range order as the particle concentration increased. These studies have demonstrated the effectiveness of leveraging the rich phase behavior of block copolymers in obtaining a periodic distribution of the magnetic nanoparticles within polymer matrices. In addition, a hybrid morphology can be designed based on the current understanding of the phase behavior of block copolymers and magnetic nanoparticle mixtures.

This study investigated the effects of the molecular weight of the polymer and the rod concentration on the dispersion of magnetic nanorods in homopolymers and block copolymers. Compared with magnetic nanospheres, magnetic nanorods are more functional because they potentially provide unique properties attributable to their anisotropic morphology.[43,44] The magnetic moments of magnetic nanorods arranged into planar arrays in a side-by side manner exhibit antiferromagnetic coupling, whereas the magnetic moments of nanorods connected in an end-to-end fashion exhibit ferromagnetic coupling.[45] Thus, to induce large shape anisotropy among magnetic nanorods, the spatial distribution of the nanorods must be controlled. Although the dispersion of magnetic nanospheres in polymer matrices has been documented extensively, the current knowledge on the organization of magnetic nanorods in block copolymers is limited.[46] We considered composites composed of pyridine-modified magnetic nanorods and polymers, namely, poly(2 vinylpyridine) (P2VP) homopolymers and poly(styrene-*b*-2 vinylpyridine) (PS-P2VP) diblock copolymers. The structural characteristics of nanocomposites and the dispersion of nanorods were determined using transmission electron microscopy (TEM) and small angle X-ray scattering (SAXS). Our results clearly illustrated the effect of the molecular weight of the polymer on the stability of magnetic nanorods in polymer matrices. The phase behavior of the nanocomposites resulted from the interplay between attractive interparticle interactions, the preferential interaction between the pyridine-modified nanorods and the P2VP blocks, and the entropic effects within the copolymer. Because few studies have provided both experimental and theoretical data on the phase behavior of polymer/magnetic nanorod composites, this paper provides essential guidance in identifying the key physical variables that can be used to disperse particles uniformly and control polymer morphology.

EXPERIMENTAL SECTION

Preparation of magnetic nanorods

Fe_2P nanorods were prepared using a method described in the literature.[47] In brief, a mixture of 0.3 g of $Fe(CO)_5$ (>97%, Sigma-Aldrich Co.) and 4.8 g of trioctylphosphine (TOP, Sigma-Aldrich Co.) was prepared at 100 °C. The stock solution was quickly injected into 5.0 g of preheated trioctylphosphine oxide (TOPO, Sigma-Aldrich Co.) at 340 °C in an argon atmosphere. Further reaction for 10 min yielded the Fe_2P nanorods, which were purified through precipitation in excess acetone several times to remove the residual ions and unreacted chemicals.

The pyridine-modified Fe_2P nanorods were prepared according to the ligand exchange process described by Gupta *et al.*[48] Alkane-covered rods were refluxed in 10 ml of anhydrous pyridine (Sigma-Aldrich Co.) at 100 °C for 24 h. Excess acetone was subsequently added to the mixture, and the nanorods were precipitated through centrifugation. The purification procedure was repeated several times, and then the nanorods were redispersed in tetrahydrofuran (THF, approximately 100%, J. T. Baker). Fourier transform infrared

This article is copyrighted as indicated in the article. Reuse of AIP content is subject to the terms at: http://scitation.aip.org/termsconditions. Downloaded to IP: 140.110.200.41 On: Thu, 31 Dec 2015 02:28:59

(FTIR) spectra of TOPO- and pyridine-tethered nanorods were obtained in dried KBr powder using a JASCO spectrometer model FT/IR 4100. Thermal gravimetrical analysis (TGA) was performed using the Perkin-Elmer TGA-7 to determine the amount of pyridine covered on the rod surface. The residue during thermal analysis was assumed to be the amount of the pure nanorods. The areal density of ligands on the rod surface was determined by dividing the number of ligands per rod by the average surface area of the rods.[49,50] The lengths and diameters of the magnetic nanorods were characterized by performing TEM using a Hitachi H7500 electron microscope. The samples subjected to TEM analysis were prepared by dispersing a drop of the nanorods in THF on a copper grid coated with a carbon film. For statistical purposes, the average size and shape distribution were determined by counting several hundred particles.

Preparation and characterization of polymer/nanorod composites

The as-prepared nanorods were mixed with various polymers in THF to prepare the nanocomposites. Table I lists the molecular properties of these polymers. The complex solution was stored under ambient conditions for at least 2 days. The nanocomposites were embedded in epoxy and cast on Kapton. The samples were then dried under ambient conditions and subsequently subjected to thermal annealing in a vacuum oven at 180 °C for 5 days. For TEM analysis, an Ultracut R microtome (Reichert, Leica, MI) was used to section the embedded samples in epoxy to a thickness of approximately 80 nm. In PS-P2VP/nanorod composites, the P2VP domains were stained selectively using an iodine vapor for 24 h to enhance the contrast between the PS domain and P2VP domain. The morphology of the nanocomposites was then characterized using TEM. The images were acquired over various areas of the same and duplicate specimens.

To complement the TEM results, SAXS measurements were performed both at Sector 23A1 at the National Synchrotron Radiation Research Center in Taiwan and using a Bruker diffractometer (NanoSTAR U System, Bruker AXS Gmbh, Karlsruhe, Germany). Samples on Kapton were measured at room temperature at a sample-to-detector distance of 2 m. The data were corrected for incident flux, absorption, detector sensitivity variation, and dark current.

RESULTS AND DISCUSSION

Characterization of nanorods

Figure 1(a) shows the magnetic nanorods synthesized using thermal decomposition. Figures 1(b)-1(d) summarizes the length, diameter, and aspect ratio of the nanorods, respectively. These nanorods had the average length of 23.0 ± 3.0 nm and the average diameter of 6.1 ± 1.1 nm. The areal density of pyridine chains on the rod surface was 0.76 chains/nm^2.

Figure 2 shows the synthesized nanorods before and after surface modification. Before the ligand exchange process, the strong C–H bands occurred at 2860 cm^{-1} and 2930 cm^{-1} were observed, which was contributed by TOPO. After the replacement of TOPO by pyridine, the signal of C–H bands decreased considerably. Additionally, two pronounced peaks arising from the adsorbed pyridine on the rod surface appeared at approximately 1720 cm^{-1} and 1600 cm^{-1}, which were assigned to the stretching vibrations of C=C and C=N, respectively. These FTIR results confirmed that the nanorods were modified effectively by pyridine.

Dispersion of nanorods in homopolymers

To fully understand the miscibility of the pyridine-modified nanorods within the P2VP domains in block copolymers, we first investigated the dispersion of the nanorods in P2VP homopolymers. Figure 3 shows cross-sectional TEM images of nanorods in P2VP with a molecular weight of 7300 g/mol. To categorize the dispersion state of the nanorods in P2VP, we used the definition presented by Hore *et al.*:[51] dispersed system when more than 90% of the nanorods are isolated from each other, partially aggregated system when the fraction of isolated nanorods is between 50% and 90%, and aggregated system when less than 50% of the nanorods are isolated. When the weight fraction of nanorods (ϕ) was 0.5%, the nanorods aggregated, indicating that phase separation occurred. This phase separation suggested that the miscibility of the P2VP/nanorod mixture was poor. The nanorods remained aggregated as the rod concentration was increased, and the aggregates increased in size as the weight fraction of the nanorods increased. The nanorods eventually aggregated extensively forming a loosely packed structure at ϕ = 5.0%.

Figure 4 shows the representative TEM images of nanorods organized in P2VP with a molecular weight of

TABLE I. Characteristics of polymers.

Polymer[a]	M_n of PS (g/mol)[b]	M_n of P2VP (g/mol)[b]	PDI[c]	D (nm)[d]
P2VP		7300	1.14	
		40600	1.09	
		110000	1.60	
PS-P2VP	8200	8300	1.09	17.3
	40500	40000	1.10	55.2
	75000	66500	1.15	67.9
	10200	97000	1.12	75.2

[a]All the polymers were purchased from Polymer Source, Inc.
[b]M_n is the number-averaged molecular weight.
[c]PDI is the polydispersity index.
[d]Lamellar periods were determined by SAXS.

This article is copyrighted as indicated in the article. Reuse of AIP content is subject to the terms at: http://scitation.aip.org/termsconditions. Downloaded to IP: 140.110.200.41 On: Thu, 31 Dec 2015 02:28:59

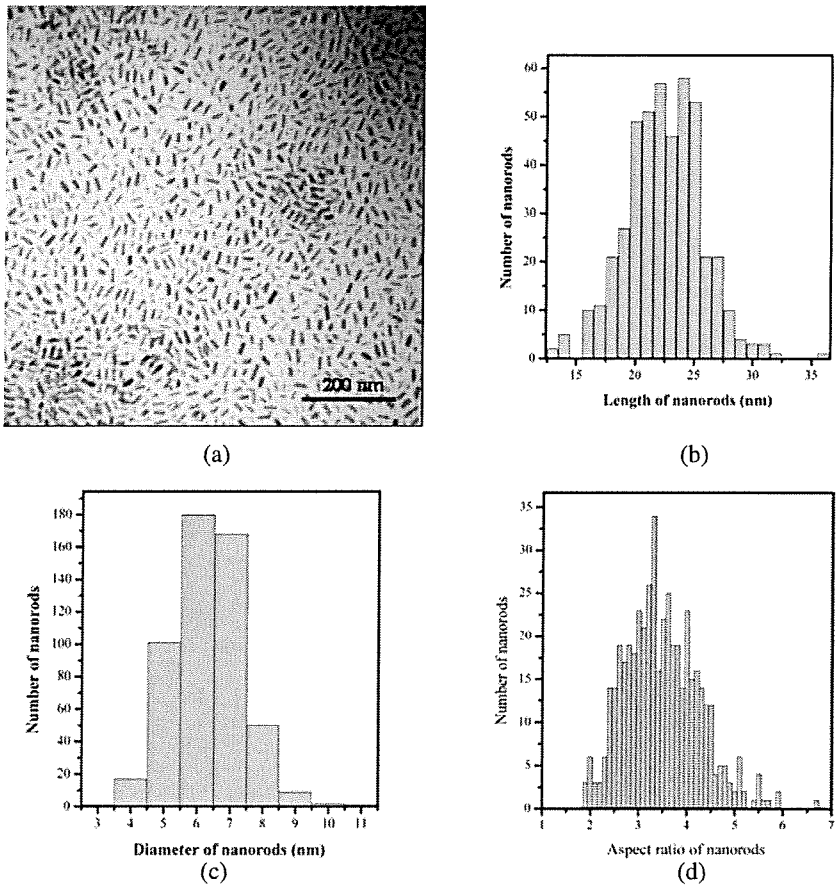

FIG. 1. (a) TEM image of the synthesized nanorods; (b) length distribution; (c) diameter distribution; and (d) aspect ratio distribution.

40 600 g/mol. In this system, $R_{g,rod}$ was nearly identical to $R_{g,P2VP}$. At $\phi = 0.5\%$ and 1.0%, the nanorods were uniformly dispersed. This thermally stable phase behavior enabled the nanorods to swell the P2VP chains, resulting in an entropic penalty attributable to the chain stretching caused by the accommodation of nanorods. However, the increase in the translational entropy of nanorods caused by particle dispersion can compensate for the loss of conformational entropy. When additional nanorods were added, they tended to form irregular aggregates with equivalent sizes, which were slightly less than 200 nm.

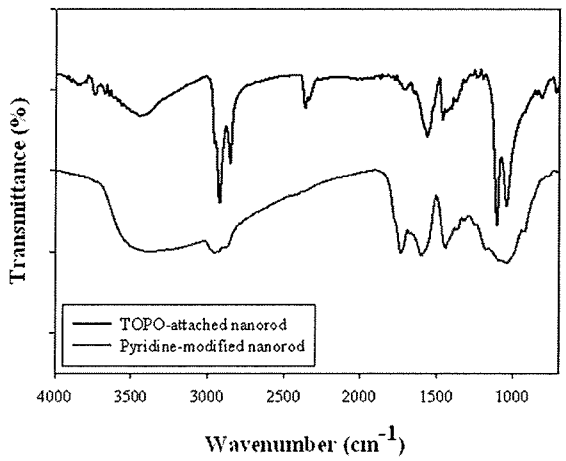

FIG. 2. FTIR of the synthesized nanorods.

Figure 5 shows the dispersion of nanorods in P2VP with a molecular weight of 110 000 g/mol. When low numbers of nanorods were incorporated into P2VP (Figures 5(a) and 5(b)), no rod aggregation occurred. At $\phi = 2.5\%$, loosely packed clusters containing few nanorods developed and coexisted with isolated nanorods, meaning that the nanorods were partially aggregated. All clusters were smaller than 100 nm. When ϕ reached 5.0 wt. %, as shown in Figure 4(d), irregular aggregates formed, which is similar to that obtained when nanorods were mixed with P2VP with a molecular weight of 40 600 g/mol at a high particle loading.

The dispersion of nanoparticles in a polymer depends on various parameters, including the sizes and shapes of the particles, the radius of gyration of the polymer, the interaction between particles and the polymer, the grafting density of ligands on the particle surface, and the relative molecular weight of the polymer and the brushes. To obtain thermodynamically stable dispersion of spherical nanoparticles in a polymer matrix, a general approach is to modify the surface of the nanoparticles by grafting polymers or ligands that are compatible to the polymer matrix, resulting in a brush that can effectively shield the particles and prevent them from aggregation. In particular, the degree of polymerization of the grafting polymers needs to be greater than that of the polymer matrix to create a condition of a wet brush.[37,52] In the mixture of polymers and nanorods, Hore *et al.* suggested

This article is copyrighted as indicated in the article. Reuse of AIP content is subject to the terms at: http://scitation.aip.org/termsconditions. Downloaded to IP: 140.110.209.41 On: Thu, 31 Dec 2015 02:28:59

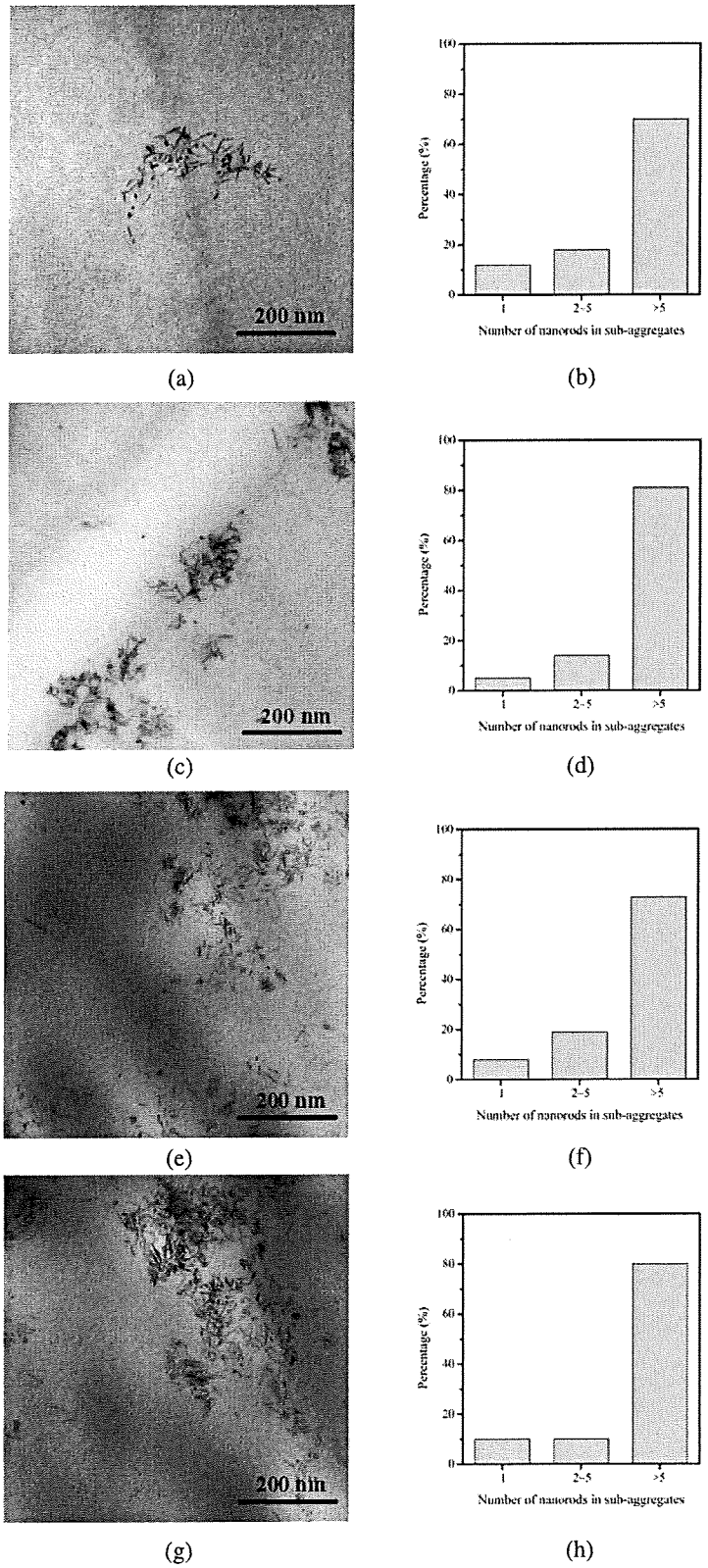

FIG. 3. The dispersion of nanorods in P2VP with a molecular weight of 7300 g/mol. ((a) and (b)) $\phi = 0.5\%$; ((c) and (d)) $\phi = 1.0\%$; ((e) and (f)) $\phi = 2.5\%$; and ((g) and (h)) $\phi = 5.0\%$.

that the dispersion of nanorods was achieved when the degree of polymerization of grafting polymers was greater than twice that of the polymer matrix.[51,53] When nanorods were confined in a thin film architecture, nanorods were aligned parallel to the film at low particle concentration.[54] By contrast, nanorods formed aggregates containing side-by-side arrays with increasing particle concentration. Although these studies successfully demonstrate the dispersing of nanoparticles in polymers by the use of long grafts for nanoparticles, these long grafts can cause a substantial increase in the effective

This article is copyrighted as indicated in the article. Reuse of AIP content is subject to the terms at: http://scitation.aip.org/termsconditions. Downloaded to IP: 140.110.200.41 On: Thu, 31 Dec 2015 02:28:59

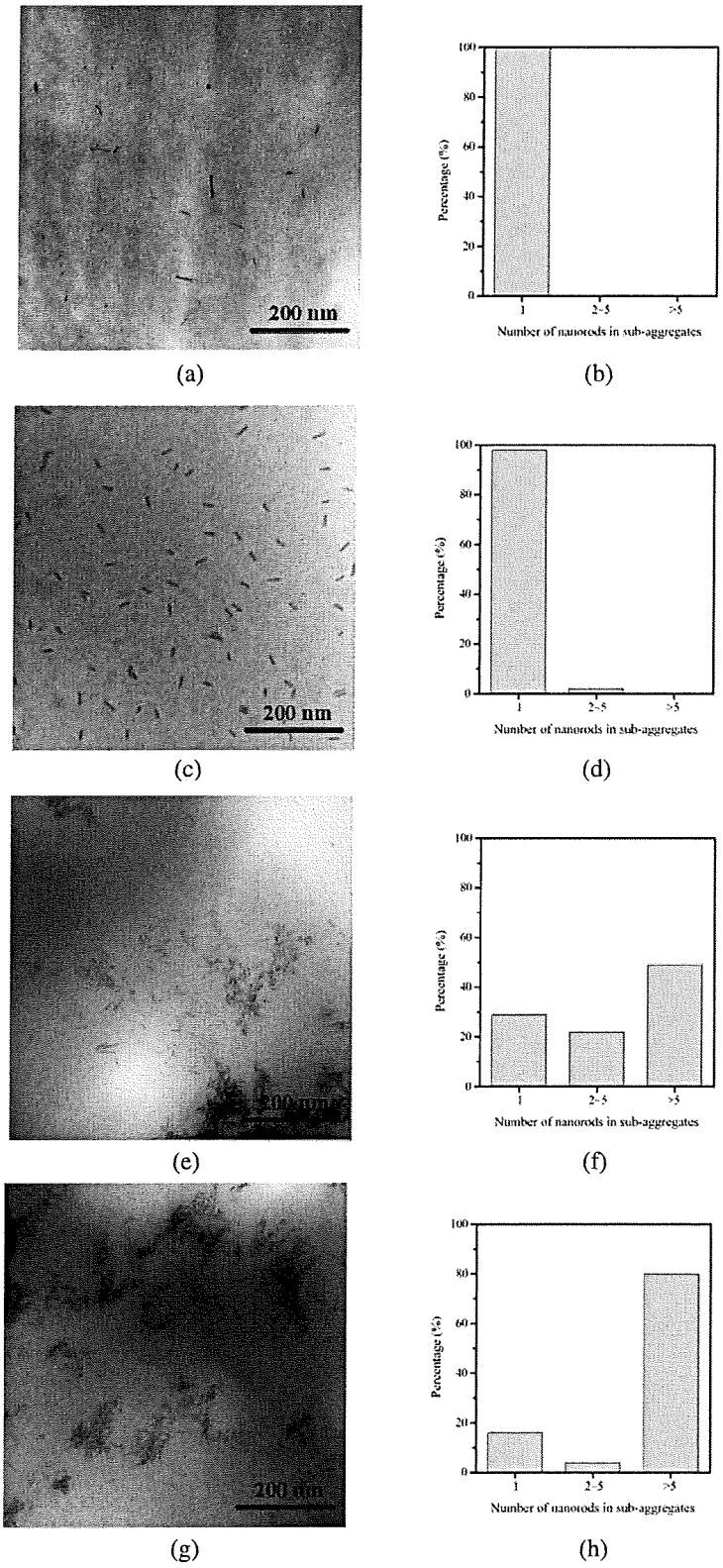

FIG. 4. The dispersion of nanorods in P2VP with a molecular weight of 40 600 g/mol. ((a) and (b)) $\phi = 0.5\%$; ((c) and (d)) $\phi = 1.0\%$; ((e) and (f)) $\phi = 2.5\%$; and ((g) and (h)) $\phi = 5.0\%$.

size of the nanoparticles. This reduces the achievable concentration of the nanoparticles in the polymer and affects physical properties of the nanocomposites. By using molecular dynamics simulations, Smith and Bedrov demonstrated that the repulsive interactions between nanoparticles could be achieved even when polymer grafts were much shorter than polymer matrices.[55] Mackay *et al.* used polymeric nanoparticles addressed the criteria for the miscibility of the non-tethered nanoparticles in a polymer matrix, stating that the dispersion of particles is uniform when the radius of gyration of the polymer is greater than that of the particles.[56] Regarding rod-shaped particles, theoretical calculations suggested that

This article is copyrighted as indicated in the article. Reuse of AIP content is subject to the terms at: http://scitation.aip.org/termsconditions. Downloaded to IP: 140.110.200.41 On: Thu, 31 Dec 2015 02:28:59

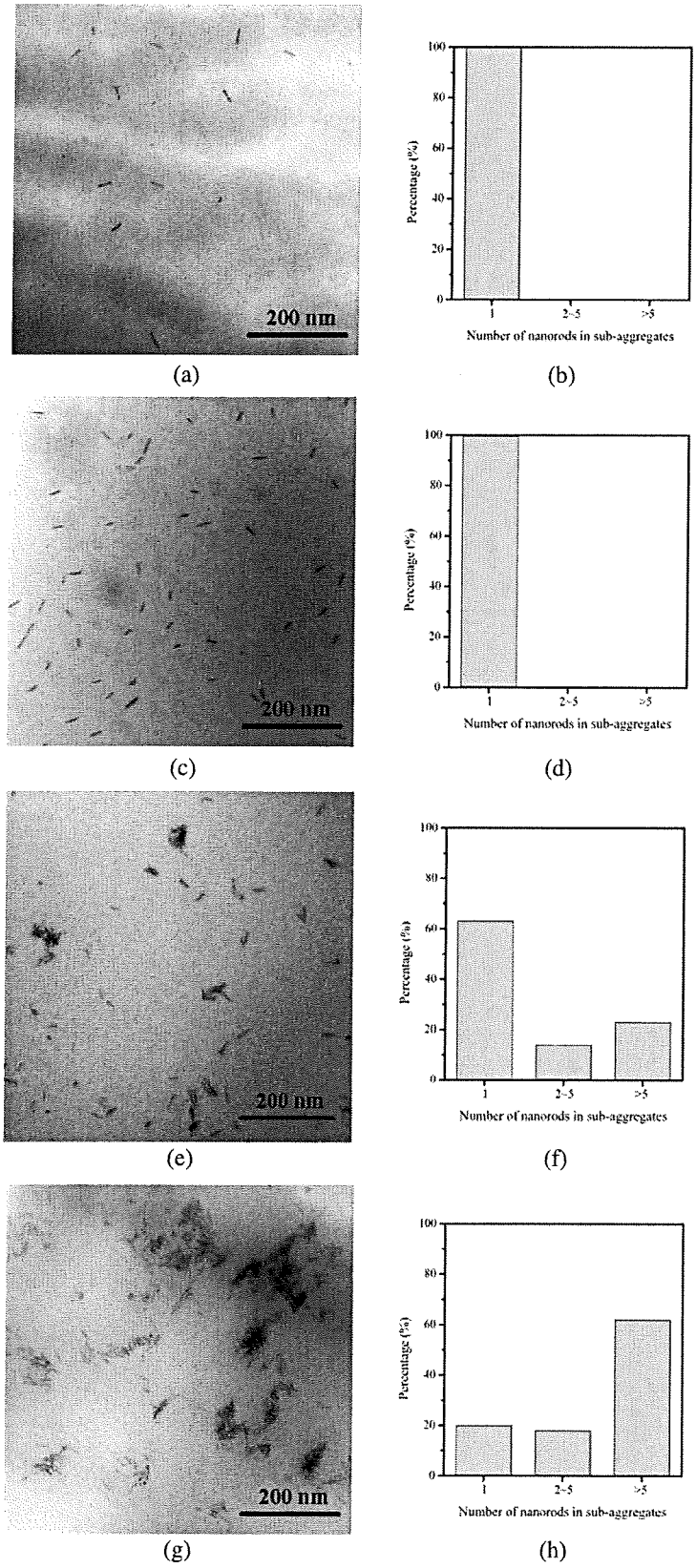

FIG. 5. The dispersion of nanorods in P2VP with a molecular weight of 110 000 g/mol. ((a) and (b)) $\phi = 0.5\%$; ((c) and (d)) $\phi = 1.0\%$; ((e) and (f)) $\phi = 2.5\%$; and ((g) and (h)) $\phi = 5.0\%$.

the polymer-induced repulsive interactions provided steric stabilization, which could outweigh short-range attractions, preventing aggregation of hard nanorods.[57,58] Similar behavior was reported by a study in which a large radius of gyration of polymer and a small rod radius facilitated rod dispersion.[59] However, this result was obtained without considering the effect of rod length on rod dispersion. As mentioned previously, the dispersion of particles caused chain stretching, which was

This article is copyrighted as indicated in the article. Reuse of AIP content is subject to the terms at: http://scitation.aip.org/termsconditions. Downloaded to IP: 140.110.200.41 On: Thu, 31 Dec 2015 02:28:59

followed by the loss of conformational entropy. Although nanorods with a large radius caused polymer molecules to stretch, long nanorods mainly increased the number of stretched chains because the contact area with polymer molecules was increased, suggesting that the particle size effect cannot be simplified easily by using only one dimension for anisotropic particles. Thus, an experimental study proved that long nanorods exert substantial influence in inducing extensive aggregation when dispersed in a polymer matrix.[46] A computational method also predicted that increasing the rod length resulted in strong depletion attractions, which induced immiscibility between the nanorods and polymer matrix.[57] In this study, we fixed the size of nanorods and varied the molecular weight of P2VP. Our results suggested that, when the molecular weight of P2VP was low, the polymer media imposed a severe entropic penalty and nanorods were excluded from the polymer chains, inducing extensive aggregation. The dispersion of nanorods greatly improved when the molecular weight of P2VP increased, which could be attributed to the steric hindrance contributed from the high molecular weight of P2VP. Although differences in the system parameters, such as the particle shape and the interparticle interaction, existed between our study and those of the literature reports,[56–60] we mixed nanorods in a polymer with a high molecular weight to achieve a uniform dispersion, thus validating the stability criteria proposed by these literatures.

Self-assembly of nanorods in block copolymers

This section describes the incorporation of the pyridine-modified magnetic nanorods into the P2VP domains of symmetric PS-P2VP. This process was facilitated by preferential interaction between ligands and P2VP. All neat PS-P2VP block copolymers exhibited a lamellar structure, enabling the effect of morphology on rod dispersion to be ignored. Although the physics of polymer stretching and interparticle interactions in mixtures of nanorods and P2VP and mixtures of nanorods and PS-P2VP are expected to be similar, the rod dispersion in block copolymers is more complex because new features associated with the confinement effect in lamellae formed by diblock species are involved.

Figure 6 shows the dispersion state of nanorods in PS-P2VP with a molecular weight of 8200–8300 g/mol. In the micrographs, the white areas are the segregated PS sequences, the grey areas are the P2VP phase, and the black spots are composed of nanorods. The neat PS-P2VP in Figure 6(a) clearly indicates the formation of a lamellar structure. When nanorods were added, they formed particle-rich regions. Because the size of rod aggregates suppressed the domain size of P2VP, these aggregates failed to become incorporated into the preferred domains of P2VP, causing macrophase separation. The phase separation of nanorods and PS-P2VP remained at a high particle loading.

To complement the phase behavior of PS-P2VP/nanorod composites, we used SAXS to determine the structural features of these nanocomposites, as shown in Figure 6(f). The SAXS profiles show that the neat PS-P2VP exhibited diffraction peaks with a ratio of the peak position of 1:3, indicating the formation of a lamellar structure. The absence of even-order reflections is due to the symmetry grounds for symmetric diblocks where the sublayers had nearly equal thickness. The intensity of the diffraction peaks decreased substantially as nanorods were added; this observation was associated with the decreased ordering of polymer microdomains. In addition, the strong scattering signal emitted by the nanorods masked the signal of the structure factors from the ordered phases of PS-P2VP.[61] This effect was pronounced, especially in the high q region (scattering vector, where $q = 4\pi\sin(\theta/2)/\lambda$, θ is the scattering angle, and λ is the incident radiation wavelength). However, at $\phi = 5.0\%$, the first order peak was still visible, indicating that the lamellar phase of PS-P2VP coexisted with aggregated nanorods, and the SAXS results exhibited strong consistency with the micrographs obtained using TEM.

Figures 7 and 8 show the phase behavior of the PS-P2VP/nanorod composites with a molecular weight of PS-P2VP of 40 500–40 000 and 75 000–66 500 g/mol, respectively. Again, the nearly symmetric PS-P2VP phase separated into a lamellar structure. When nanorods were incorporated into PS-P2VP, the nanorods were sequestered into the P2VP domains without disturbing the morphology of PS-P2VP. The particle dispersion was uniform at a low particle concentration. With increasing particle concentration, the segregation of nanorods in the PS domains increased, indicating that the particle selection in the preferred domains of PS-PVP reduced. At $\phi = 1.0\%$ for PS-P2VP with M_n of 40 500–40 000 g/mol and $\phi = 2.5\%$ for PS-P2VP with M_n of 75 000–66 500 g/mol, the solvophilicity of nanorod declined, causing small aggregates to form. Most of these aggregates had the equivalent size comparable to the P2VP domain size, and the aggregates were still capable of being confined in the P2VP domains. Increasing particle loading further caused extensive aggregation, but the ordered polymer phases remained unchanged. The SAXS profiles in Figures 7(f) and 8(f) confirm the TEM results. For neat PS-P2VP, several peaks, including higher-order reflections, were observed, indicating the development of highly ordered phases. The higher-order peaks gradually became smeared as nanorods were added because of particle scattering. In addition, the lower-order peaks broadened; this observation was attributed to the addition of nanoparticles, which caused the variation in the domain size, defects at domain boundaries, and interfacial roughness.[41] When the rod concentration was high, a structure factor appeared at $q \approx 0.08$ Å^{-1}, indicating the interparticle correlation caused by rod aggregation.

Figure 9 shows the phase behavior of the mixture of nanorods and PS-P2VP with a molecular weight of 102 000–97 000 g/mol. Similar to the PS-P2VP with a medium molecular weight (PS-P2VP = 40 500–40 000 and 75 000–66 500 g/mol), the incorporation of nanorods in this PS-P2VP exhibited favorable selection of nanorods in the P2VP domains, particularly nanorods aligned parallel to the interface between PS and P2VP. We define an alignment of the long axis of nanorods along the PS-P2VP interface as zero angle, and Figure 9(f) shows the orientation of nanorods at $\phi = 0.5\%$. We determined that most nanorods aligned parallel to the interface. When nanorods are oriented perpendicular to the interface, the nanorods induce local

This article is copyrighted as indicated in the article. Reuse of AIP content is subject to the terms at: http://scitation.aip.org/termsconditions. Downloaded to IP: 140.113.200.41 On: Thu, 31 Dec 2015 07:28:59

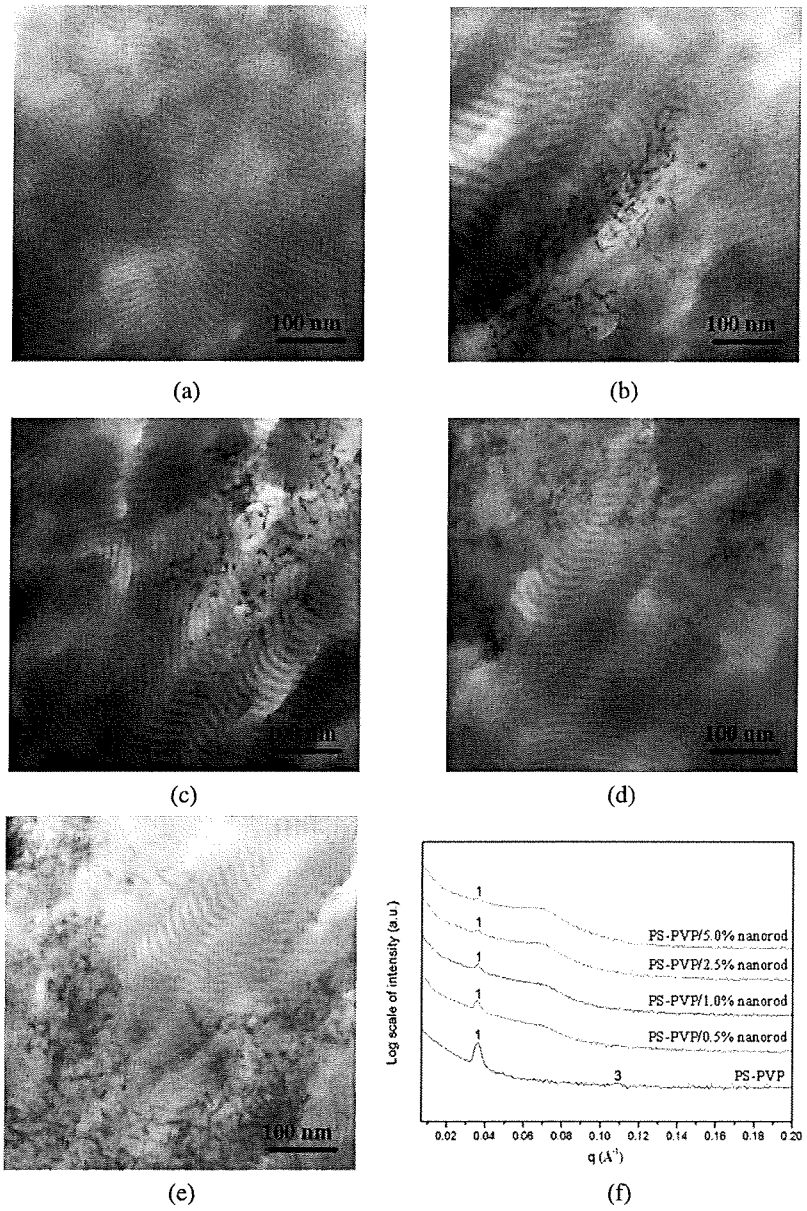

FIG. 6. TEM images of PS-P2VP/nanorod composites. (a) Neat PS-P2VP; (b) $\phi = 0.5\%$; (c) $\phi = 1.0\%$; (d) $\phi = 2.5\%$; and (e) $\phi = 5.0\%$. (f) SAXS profiles of PS-P2VP/nanorod composites. M_n of PS-P2VP is 8200–8300 g/mol.

deformation of lamellae, which amplify the compositional fluctuation between PS and P2VP interfaces, causing an excess interfacial energy. By contrast, when nanorods are aligned parallel to the interface, microdomains are relatively undistorted. This limits interfacial fluctuations, facilitating the development of the long-range order of polymer phases. The parallel alignment of nanorods with lamellae is also found in both theoretical[62–65] and experimental studies.[46,66] At ϕ = 5.0%, extensive aggregation was observed. Although rod aggregation occurred, numerous nanorods still dispersed in the PS-P2VP without a preferred location, forming a mixture of isolated and aggregated nanorods. Figure 9(g) shows the SAXS data on the high-molecular-weight PS-P2VP and high-molecular-weight PS-P2VP/nanorod composites. All of the nanocomposites exhibited an ordered morphology. The interparticle correlation decreased when compared with that in the composites composed of low-molecular-weight PS-P2VP, suggesting that the nanorods dispersed more uniformly in the high-molecular-weight PS-P2VP. From the SAXS data, the domain size of the composites calculated by the Bragg law increased from 75.2 nm for the neat PS-P2VP to 75.8 nm, 76.4 nm, and 77.2 nm for 0.5%, 1%, and 2.5% nanorods, respectively. The monotonic increase in the domain size was caused by the effect of the axial expansion of the P2VP domain with the addition of the nanorods.

Histograms of particle center location as a function of the distance from the center of the polymer interface are shown in Figure 10. When M_n of PS-P2VP was 102 000–97 000 g/mol, a large amount of the nanorods were concentrated in the P2VP domains, particularly near the edge of the interface between the PS and P2VP domains (Figure 10(b)). However, we also observed some nanorods distributed in the energetically unfavorable PS domains. Decreasing the molecular weight of PS-P2VP facilitated the segregation of the nanorods to the center of the P2VP domains. He *et al.* used the dissipative particle dynamics simulations to investigate the mesophase

This article is copyrighted as indicated in the article. Reuse of AIP content is subject to the terms at: http://scitation.aip.org/termsconditions. Downloaded to IP: 140.110.200.41 On: Thu, 31 Dec 2015 02:28:59

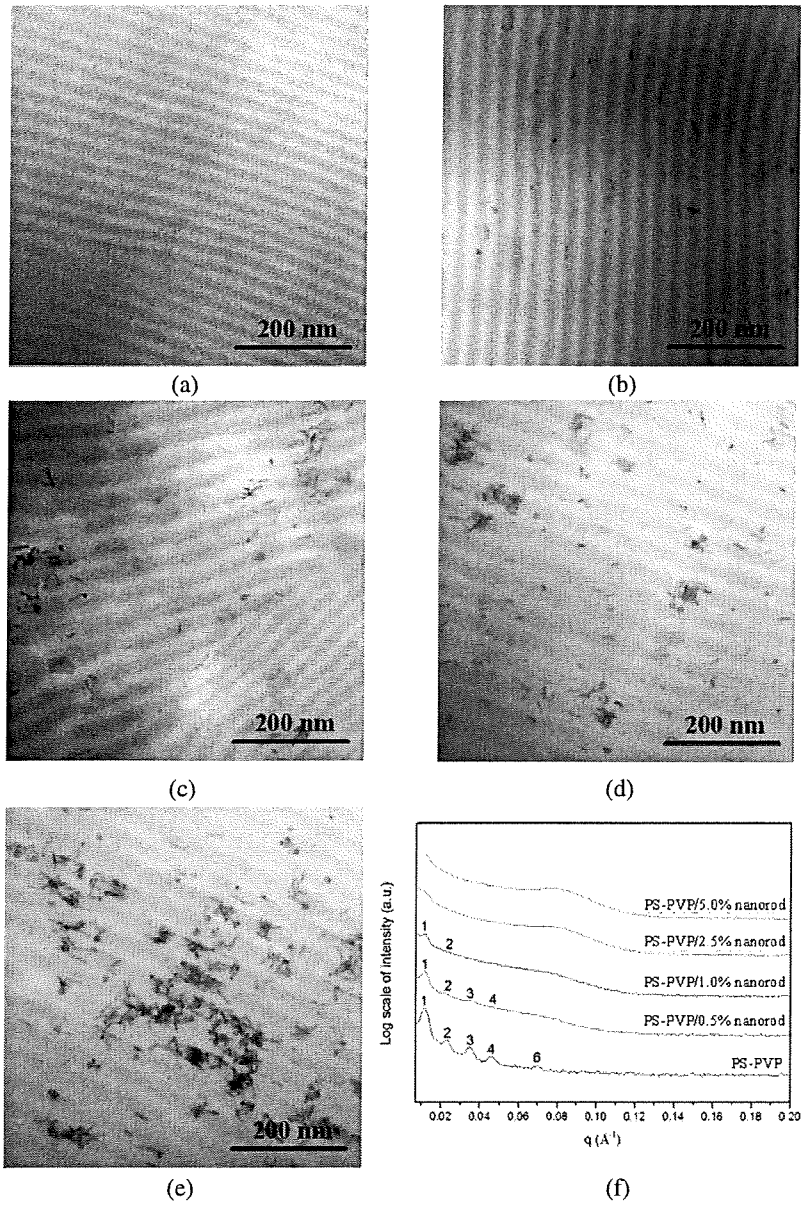

FIG. 7. TEM images of PS-P2VP/nanorod composites. (a) Neat PS-P2VP; (b) $\phi = 0.5\%$; (c) $\phi = 1.0\%$; (d) $\phi = 2.5\%$; and (e) $\phi = 5.0\%$. (f) SAXS profiles of PS-P2VP/nanorod composites. M_n of PS-P2VP is 40 500–40 000 g/mol.

structure formed in the mixture of block copolymer and nanorods.[62] By assigning a constant rod diameter and domain period, they found that long nanorods tended to locate at the center of the preferred domains to maintain the conformational entropy of the favorable domain. By contrast, short nanorods gained their maximum translational entropy via organizing at the polymer interface. In our study, the rod length was smaller than the domain size of P2VP with the molecular weight of 102 000–97 000 g/mol, and the dispersion of the nanorods is consistent with the short-rod case predicted in the simulation.[62] When the molecular weight of PS-P2VP was changed to 40 500–40 000 g/mol, the rod length was comparable to the P2VP domain size, and the dispersion of the nanorods behaved as the long nanorods in block copolymer. This entropic-driven particle organization has also been observed in the mixture of block copolymer and spherical nanoparticles.[67]

Based on the results regarding the assembly behavior of the nanorods in PS-P2VP, we categorized the organization of nanorods into three classes, namely, uniform dispersion, small aggregates (aggregate size $\leq$ 100 nm), and large aggregates (aggregate size > 100 nm). The phase behavior of block copolymer/magnetic nanorod composites is summarized in Figure 11 according to these definitions. The behavior was correlated with the lamellar period of the neat block copolymer (D), which was determined using the equation $2\pi/q_1$ where q_1 is the position of the first-order reflection in SAXS. The phase diagram reveals that the critical concentration, at which rod aggregation was induced, decreased as the D value decreased. When D was large, the dispersion state of nanorods changed from uniform to small aggregates to large aggregates as the particle loading was increased. In this case, the size of the nanorods was relatively small, and the nanorods were able to disperse between the neighboring chains, creating a wet-brush situation. In the wet-brush regime, the dispersion of nanorods expands the preferred domains and does not diminish the conformational entropy of the system. When

This article is copyrighted as indicated in the article. Reuse of AIP content is subject to the terms at: http://scitation.aip.org/termsconditions. Downloaded to IP: 140.110.200.41 On: Thu, 31 Dec 2015 02:29:59

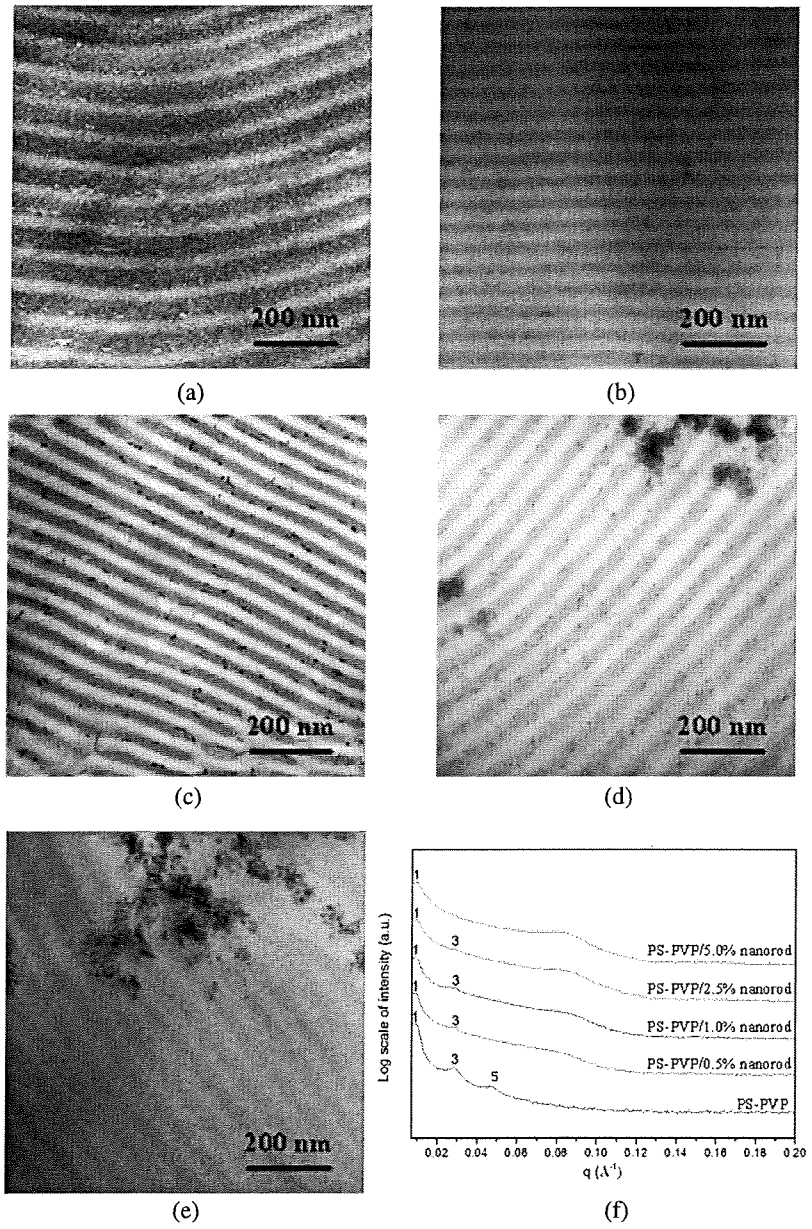

FIG. 8. TEM images of PS-P2VP/nanorod composites. (a) Neat PS-P2VP; (b) $\phi = 0.5\%$; (c) $\phi = 1.0\%$; (d) $\phi = 2.5\%$; and (e) $\phi = 5.0\%$. (f) SAXS profiles of PS-P2VP/nanorod composites. M_n of PS-P2VP is 75 000–66 500 g/mol.

D was small, the incorporation of nanorods into a confined domain causes substantial chain stretching and contraction. To regain the entropy loss, nanorods must aggregate, inducing the dry brush. This dry brush relaxes the stretched chains and expels nanorods from the ordered domains. Consequently, rod aggregation was observed even at a low particle loading. Our results of the rod dispersion under confinement agree well with the behavior of the magnetic nanorods in a lamellar lyotropic phase.[68]

Regarding the dispersion of nanorods in one domain of a block copolymer, the introduction of nanorods caused chain stretching and contraction, as mentioned in the previous paragraphs in the section "Self-assembly of nanorods in block copolymers." When nanorods were under confinement, the stretched chains were relaxed as the preferred domain size increased (Figure 12(a)), indicating that using high-molecular-weight block copolymers and nanorods with small radii facilitates rod dispersion. We previously investigated the effect of rod length on the dispersion of nanorods in block copolymers while keeping the rod radius constant.[46] It was obtained that using long nanorods increased the number of stretched chains, as shown in Figure 12(b). Therefore, incorporating long nanorods into block copolymers is energetically unfavorable. Based on our present findings, a uniform dispersion of nanorods is generally achieved when both D is large and ϕ is low. Either decreasing the D or increasing the ϕ value reduces the compatibility of the system, and a two-phase coexistence consisting of macroscopically phase-separated rod aggregates and block copolymers develops. In addition, the size of the particle aggregates increases as the value of D decreases or ϕ increases. By tuning the system parameters, uniform dispersed nanorods can be achieved when the D value is larger than 67.9 nm and the ϕ value is 1 wt. %. This D value is much greater than both the radii and

This article is copyrighted as indicated in the article. Reuse of AIP content is subject to the terms at: http://scitation.aip.org/termsconditions. Downloaded to IP: 140.110.200.41 On: Thu, 31 Dec 2015 02:28:59

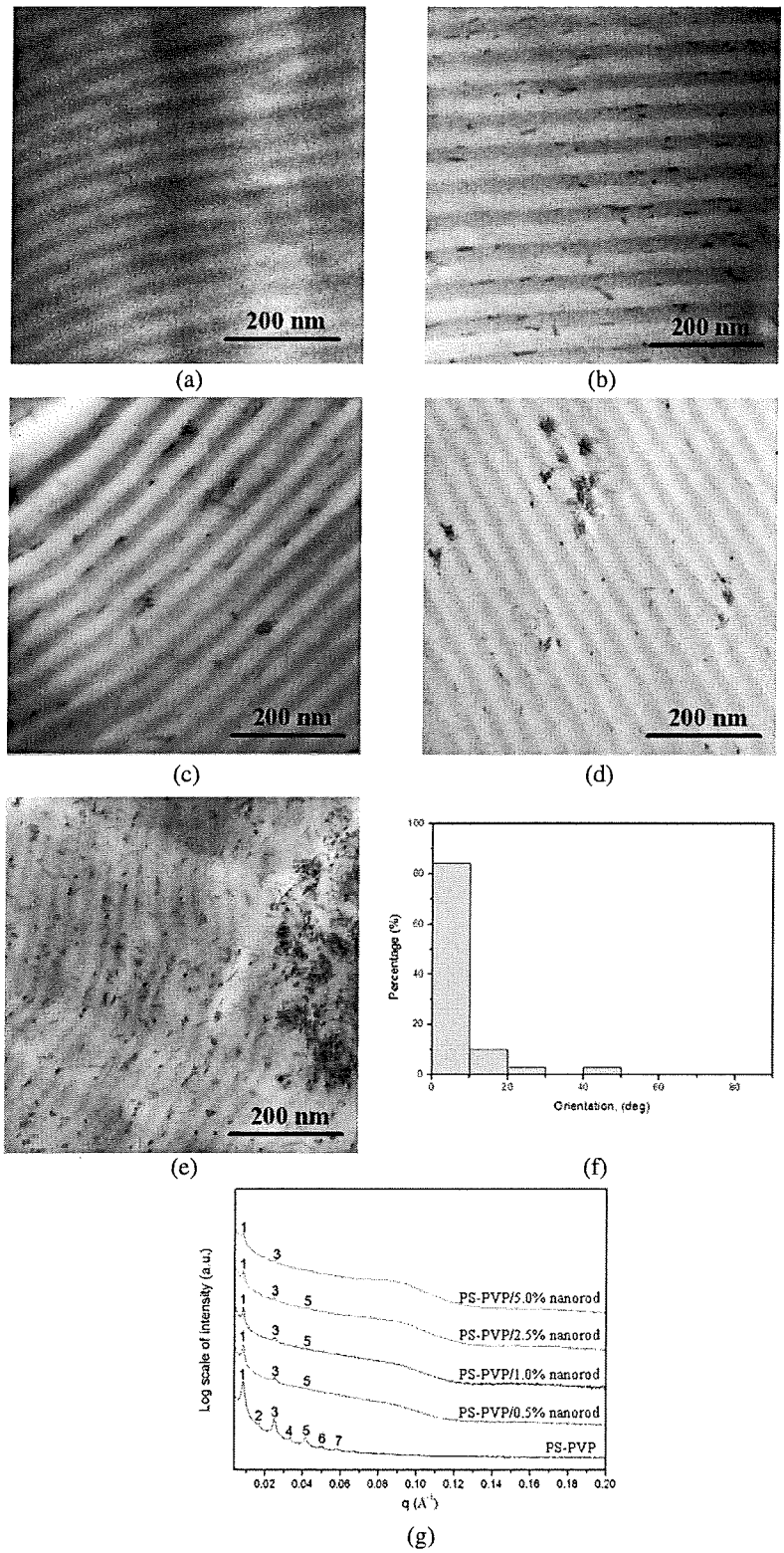

FIG. 9. TEM images of PS-P2VP/nanorod composites. (a) Neat PS-P2VP; (b) $\phi = 0.5\%$; (c) $\phi = 1.0\%$; (d) $\phi = 2.5\%$; and (e) $\phi = 5.0\%$. (f) Orientation of nanorods in PS-P2VP at $\phi = 5.0\%$ and (g) SAXS profiles of PS-P2VP/nanorod composites. M_n of PS-P2VP is 102 000–97 000 g/mol.

length of the nanorods. Xu *et al.* demonstrated the assembled behavior of magnetite nanospheres in block copolymers.[38] At $\phi = 1$ wt. %, the nanoparticles, of which the radius of nanospheres (R_{sphere}) and D was 2.5 and 34.2 nm, dispersed selectively in the preferred domains of the block copolymer. By contrast, nanoparticles formed small aggregates at $\phi = 4$ wt. %. Wu *et al.* incorporated iron oxide nanospheres into the middle domain of poly(styrene-butadiene-styrene) triblock copolymers.[41] Although the middle block in triblock copolymers has no free chain end (unlike diblock copolymers, which have one free chain end), the organization of nanorods varied substantially according to the R_{sphere} and D values.

This article is copyrighted as indicated in the article. Reuse of AIP content is subject to the terms at: http://scitation.aip.org/termsconditions. Downloaded to IP: 140.110.200.41 On: Thu, 31 Dec 2015 02:28:59

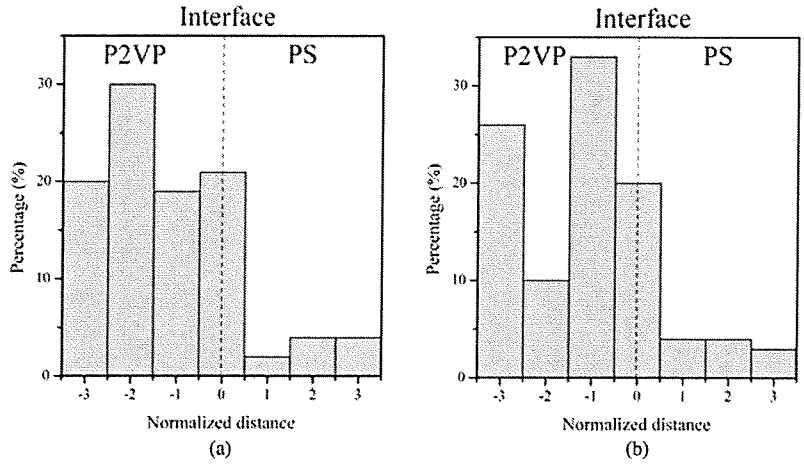

FIG. 10. Location of nanorods in the microdomains of PS-P2VP. (a) M_n = 40 500–40 000 g/mol and (b) M_n = 102 000–97 000 g/mol. The weight fraction of nanorods is 0.5%. Data are normalized at a given position relative to the interface.

When R_{sphere} was 4.1 nm ($D \approx 30$ nm according to TEM), the particles were confined in the center of the polybutadiene layers at a low particle concentration, whereas the particles formed long strings at a high particle concentration because of the strong magnetic interactions. By contrast, when R_{sphere} was 7.6 nm, the particles formed aggregates with 100–300 nm in size. These studies suggested the importance of the relative size between the R_{sphere} and D values on the dispersion of nanospheres. Compared with the isotropic particles, mixing anisotropic particles in a confined geometry engenders an additional chain conformation rearrangement. This particle shape effect may cause the decrease in the critical particle concentration at which the particle dispersion is retained. Beneut *et al.* suggested that the threshold value of the particle concentration was the order of the particle size.[68] Aggregation occurred when rotation about the long axis of the particles was hindered. Zhang *et al.* assembled noninteracting nanorods with an average length of 20–60 nm in block copolymers.[66] The nanorods were aligned along the channels generated by the lamellarly ordered block copolymer ($D \approx 60$ nm). However, the concentration of nanorods was not reported. Deshmukh *et al.* incorporated noninteracting nanorods into block copolymers.[69] At $\phi = 5$ vol. %, the nanorods with a diameter of 18.2 nm and a length of 47.7 nm were selectively segregated to the preferred domain of block copolymer (D = 67.2 nm) without the occurrence of particle aggregation. Because of considerable difference in the system parameters, direct quantitative comparison between our study and previous studies is impossible. However, we can briefly conclude that minimizing the rod size and maximizing the confined domain size are crucial to obtaining isolated particles dispersed in block copolymers. This demonstration of the relationship between the phase behavior of block copolymer/nanorod mixtures and the D or rod size is useful in predicting the morphology of polymer/nanorod composites.

In addition to the relative size of the polymer domain to the nanorods, the chemistry of the ligands on the rod surface also plays an important role on the phase behavior of block copolymer/nanorod composites. Nanorods without preference to any domains of block copolymers mainly concentrate at the interface between two blocks because of the lack of the enthalpic driving force.[63] This behavior is also found in the mixture of block copolymers and nanospheres.[70] The neutral nanoparticles have no effect on

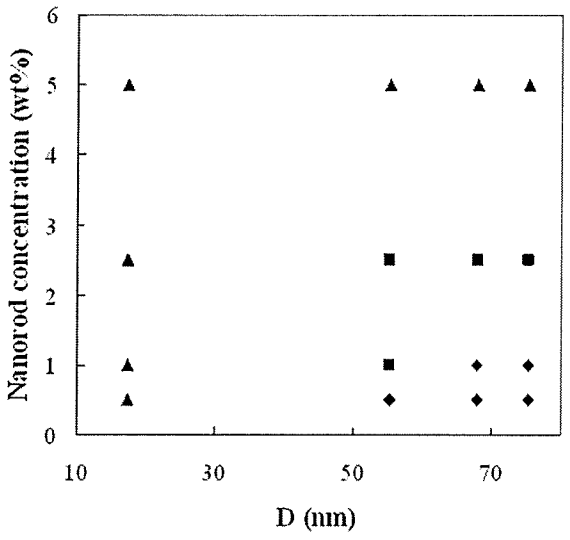

FIG. 11. The dispersion of magnetic nanorods in block copolymers (filled diamond: uniform dispersion; small clusters (≤100 nm); and large aggregates (>100 nm)).

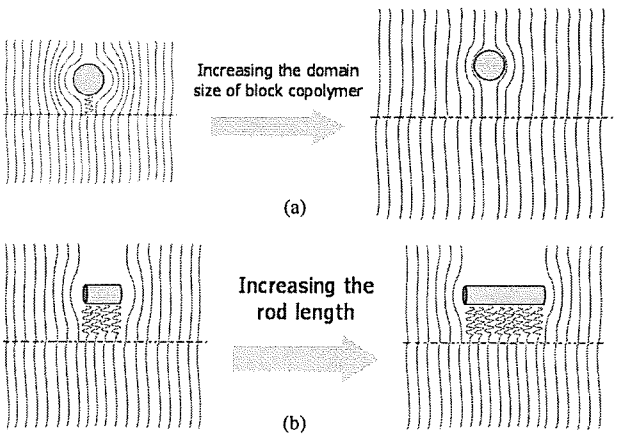

FIG. 12. Schematics of the inclusion of nanorods on perturbing the chain conformation of block copolymer. (a) Radius effect and (b) length effect.

This article is copyrighted as indicated in the article. Reuse of AIP content is subject to the terms at: http://scitation.aip.org/termsconditions. Downloaded to IP: 140.110.200.41 On: Thu, 31 Dec 2015 02:28:59

changing the morphology of block copolymers but decrease the domain size of block copolymers. By contrast, adding nanoparticles that possess a certain affinity to the preferred domain of block copolymers generally expands the preferred domains and increases the interfacial curvature, inducing an order–order transition. Theoretical studies have investigated the assembly behavior of nanorods in block copolymers, and the results suggested that the order–order transition of block copolymer microphases can be triggered effectively by the incorporating nanorods, and the stability limits of the various ordered phases can be altered by manipulating the rod length.[62–65] These studies assumed the presence of repulsive interaction between nanorods, which prevented particle aggregation and enabled the nanorods to organize in the selective domains of block copolymers. The major difference between our study and the aforementioned studies is the presence of attractive interactions between nanorods. The attractive interactions induce particle aggregation, reducing the selectivity of nanorods in the preferred domains. Thus, the volume expansion of the preferred domains caused by selective particle dispersion is limited, thereby inhibiting the morphological transition. In addition, the presence of particle aggregates enhances the effect of magnetostatic interactions, causing fluctuation between polymer interfaces.[71] This fluctuation negates the effect of polymer swelling caused by the nanorods. Consequently, the particle aggregates perturb the polymer morphology, and we observed no morphological transition in our study.

CONCLUSION

We studied the phase behavior of pyridine-modified magnetic nanorods in P2VP and PS-P2VP by using TEM and SAXS. The dispersion state of the nanorods exhibited strong dependence on the rod concentration and the molecular weight of the polymer matrix. In the mixture of a homopolymer and nanorods, the polymer matrix with a high molecular weight screened the interparticle interactions, promoting uniform rod dispersion. At a high particle loading, the nanorods organized into loosely packed clusters. Regarding the phase behavior of block copolymer/nanorod composites, particle stability resulted from interplay between interparticle attractive interactions, preferential interaction between the pyridine-modified nanorods and the P2VP blocks, and entropic effects within the copolymer. The dispersion state of the nanorods was correlated with the size of nanorods and the lamellar period of PS-P2VP. When the rod size was much smaller than the lamellar period, the nanorods could be sequestered into the P2VP domains. This enthalpically driven self-assembly was due to the preferential interaction between ligands and P2VP subchains. In addition, nanorods were aligned parallel to the interface between the P2VP and PS domains. This preferred orientation resulted from the entropically driven self-assembly that minimized the entropic penalty and eased the interfacial fluctuations. By contrast, introducing nanorods into low-molecular-weight PS-P2VP reduced the stability of the system. To accommodate nanorods, P2VP chains must be stretched, which decreases the conformational entropy. Consequently, nanorods were aggregated to regain the entropy loss thereby causing the phase separation of PS-P2VP and nanorods, forming a coexistence of polymer ordered phases and rod aggregates. We believe that our experimental findings increase the flexibility of approaches used to realize ordered spatial arrangements of magnetic nanorods within polymer matrices and provide new insight into the design of well-defined nanomaterial structures.

ACKNOWLEDGMENTS

This work was financially supported by Ministry of Science and Technology in Taiwan under Grant Nos. NSC 100-2628-E-006-001 and NSC 102-2221-E-006-018-MY3.

[1]M. H. Kryder, Proc. Electrochem. Soc. **2002-27**, 3-25.
[2]S. Sun, D. Weller, and C. B. Murray, in *The Physics of Ultra-High-Density Magnetic Recording*, edited by M. L. Plumer, J. van Ek, and D. Weller (Springer-Verlag, New York, 2001).
[3]C. T. Black, C. B. Murray, R. L. Sandstrom, and S. Sun, Science **290**, 1131 (2000).
[4]H. Gu, P.-L. Ho, K. W. T. Tsang, L. Wang, and B. Xu, J. Am. Chem. Soc. **125**, 15702 (2003).
[5]D. L. Huber, Small **1**, 482 (2005).
[6]D. W. Elliott and W.-X. Zhang, Environ. Sci. Technol. **35**, 4922 (2001).
[7]M. Takafuji, S. Ide, H. Ihara, and Z. Xu, Chem. Mater. **16**, 1977 (2004).
[8]A. E. Berkowitz, J. R. Mitchell, M. J. Carey, A. P. Young, S. Zhang, F. E. Spada, F. T. Parker, A. Hutten, and G. Thomas, Phys. Rev. Lett. **68**, 3745 (1992).
[9]S. Takahashi and S. Maekawa, Phys. Rev. Lett. **80**, 1758 (1998).
[10]A. N. Rusetski and E. K. Ruuge, J. Magn. Magn. Mater. **85**, 299 (1990).
[11]A. Jordan, R. Scholz, P. Wust, H. Fahling, and R. Felix, J. Magn. Magn. Mater. **201**, 413 (1999).
[12]E. Metallo, S. Couet, K. Schlage, R. Rohlsberger, V. Korstgens, M. Ruderer, W. Wang, G. Kaune, S. V. Roth, and P. Muller-Buschbaum, Langmuir **24**, 4265 (2008).
[13]E. Metwalli, J.-F. Moulin, J. Perlich, W. Wang, A. Diethert, S. V. Roth, and P. Muller-Buschbaum, Langmuir **25**, 11815 (2009).
[14]G. Kaune, M. A. Ruderer, E. Metwalli, W. Wang, S. Couet, K. Schlage, R. Rohlsberger, S. V. Roth, and P. Muller-Buschbaum, ACS Appl. Mater. Interfaces **1**, 353 (2009).
[15]P. Akcora, H. Liu, S. K. Kumar, J. Moll, Y. Li, B. C. Benicewicz, L. S. Schadler, D. Acehan, A. Z. Panagiotopoulos, V. Pryamitsyn, V. Ganesan, J. Ilavsky, P. Thiyagarajan, R. H. Colby, and J. F. Douglas, Nat. Mater. **8**, 354 (2009).
[16]G. A. Buxton and A. C. Balazs, Phys. Rev. E **67**, 031802 (2003).
[17]F. Du, R. C. Scogna, W. Zhou, S. Brand, J. E. Fischer, and K. I. Winey, Macromolecules **37**, 9048 (2004).
[18]G. Peng, F. Qiu, V. V. Ginzburg, D. Jasnow, and A. C. Balazs, Science **288**, 1802 (2000).
[19]G. A. Buxton and A. C. Balazs, J. Chem. Phys. **117**, 7649 (2002).
[20]L. M. Bronstein, E. S. Mirzoeva, P. M. Valetsky, S. P. Solodovnikov, and R. A. Register, J. Mater. Chem. **5**, 1197 (1995).
[21]S. Wizel, S. Margel, A. Gedanken, T. C. Rojas, A. Fernandez, and R. Prozorov, J. Mater. Chem. **14**, 3913 (1999).
[22]R. Tannenbaum, S. Reich, C. L. Flenniken, and E. P. Goldberg, Adv. Mater. **14**, 1402 (2002).
[23]A.-S. Robbes, F. Cousin, F. Meneau, F. Dalmas, R. Schweins, D. Gigmes, and J. Jestin, Macromolecules **45**, 9220 (2012).
[24]Y. Jiao and P. Akcora, Macromolecules **45**, 3463 (2012).
[25]C.-T. Lo and K.-H. Tsui, Polym. Int. **62**, 1652 (2013).
[26]E. Metwalli, V. Korstgens, K. Schlage, R. Meier, G. Kaune, A. Buffet, S. Couet, S. V. Roth, R. Rohlsberger, and P. Muller-Buschbaum, Langmuir **29**, 6331 (2013).
[27]F. S. Bates and G. H. Fredrickson, Annu. Rev. Phys. Chem. **41**, 525 (1990).
[28]B. H. Sohn and R. E. Cohen, Chem. Mater. **9**, 264 (1997).
[29]E. H. Tadd, J. Bradley, and R. Tannenbaum, Langmuir **18**, 2378 (2002).
[30]B. Hamdoun, Inorg. Mater. **40**, 949 (2004).
[31]B. Hamdoun, Eur. Polym. J. **40**, 1559 (2004).
[32]J. I. Abes, R. E. Cohen, and C. A. Ross, Mater. Sci. Eng. C **23**, 641 (2003).
[33]S. B. Darling, N. A. Yufa, A. L. Cisse, S. D. Bader, and S. J. Sibener, Adv. Mater. **17**, 2446 (2005).

This article is copyrighted as indicated in the article. Reuse of AIP content is subject to the terms at: http://scitation.aip.org/termsconditions. Downloaded to IP: 140.110.200.41 On: Thu, 31 Dec 2015 02:28:59

[34]S. B. Darling and S. D. Bader, J. Mater. Chem. **15**, 4189 (2005).
[35]M. J. Park, K. Char, J. Park, and T. Hyeon, Langmuir **22**, 1375 (2006).
[36]M. J. Park, J. Park, T. Hyeon, and K. Char, J. Polym. Sci., Part B: Polym. Phys. **44**, 3571 (2006).
[37]C. Xu, K. Ohno, V. Ladmiral, and R. J. Composto, Polymer **49**, 3568 (2008).
[38]C. Xu, K. Ohno, V. Ladmiral, D. E. Milkie, J. M. Kikkawa, and R. J. Composto, Macromolecules **42**, 1219 (2009).
[39]K. Char and M. J. Park, React. Funct. Polym. **69**, 546 (2009).
[40]C.-T. Lo and C.-J. Chao, Langmuir **25**, 12865 (2009).
[41]J. Wu, H. Li, S. Wu, G. Huang, W. Xing, M. Tang, and Q. Fu, J. Phys. Chem. B **118**, 2186 (2014).
[42]X. Xia, E. Metwalli, M. A. Ruderer, V. Korstgens, P. Busch, P. Boni, and P. Muller-Buschbaum, J. Phys.: Condens. Matter **23**, 254203 (2011).
[43]H. Zeng, J. Li, J. P. Liu, Z. L. Wang, and S. H. Sun, Nature **420**, 395 (2002).
[44]A. S. Arico, P. Bruce, B. Scrosati, J. M. Tarascon, and W. van schalkwijk, Nat. Mater. **4**, 366 (2005).
[45]F. Dumestre, B. Chaudret, C. Amiens, M. Respaud, P. Fejes, P. Renaud, and P. Zurcher, Angew. Chem., Int. Ed. **42**, 5213 (2003).
[46]C.-T. Lo and W.-T. Lin, J. Phys. Chem. B **117**, 5261 (2013).
[47]J. Park, B. Koo, K. Y. Yoon, Y. Hwang, M. Kang, J.-G. Park, and T. Hyeon, J. Am. Chem. Soc. **127**, 8433 (2005).
[48]S. Gupta, Q. Zhang, T. Emrick, and T. P. Russell, Nano Lett. **6**, 2066 (2006).
[49]B. J. Kim, J. Bang, C. J. Hawker, and E. J. Kramer, Macromolecules **39**, 4108 (2006).
[50]J. J. Chiu, B. J. Kim, G.-R. Yi, J. Bang, E. J. Kramer, and D. J. Pine, Macromolecules **40**, 3361 (2007).
[51]M. J. A. Hore, A. L. Frischknecht, and R. J. Composto, ACS Macro Lett. **1**, 115 (2012).
[52]A. L. Frischknecht, J. Chem. Phys. **128**, 224902 (2008).
[53]M. J. A. Hore and R. J. Composto, ACS Nano **4**, 6941 (2010).
[54]G. Jiang, M. J. A. Hore, S. Gam, and R. J. Composto, ACS Nano **6**, 1578 (2012).
[55]G. D. Smith and D. Bedrov, Langmuir **25**, 11239 (2009).
[56]M. E. Mackay, A. Tuteja, P. M. Duxbury, C. J. Hawker, B. van horn, Z. Guan, G. Chen, and R. S. Krishnan, Science **311**, 1740 (2006).
[57]M. Surve, V. Pryamitsyn, and V. Ganesan, Macromolecules **40**, 344 (2007).
[58]Y.-L. Lin, C.-S. Chiou, S. K. Kumar, J.-J. Lin, Y.-J. Sheng, and H.-K. Tsao, J. Phys. Chem. C **115**, 5566 (2011).
[59]A. L. Frischknecht, M. J. A. Hore, J. Ford, and R. J. Composto, Macromolecules **46**, 2856 (2013).
[60]J. U. Kim and B. O'shaughnessy, Phys. Rev. Lett. **89**, 238301 (2002).
[61]B. Lee, C.-T. Lo, S. Seifert, N. L. Dietz-Rago, R. E. Winans, and P. Thiyagarajan, Macromolecules **40**, 4235 (2007).
[62]L. He, L. Zhang, A. Xia, and H. Liang, J. Chem. Phys. **130**, 144907 (2009).
[63]L. He, L. Zhang, H. Chen, and H. Liang, Polymer **50**, 3403 (2009).
[64]L. He, L. Zhang, and H. Liang, Polymer **51**, 3303 (2010).
[65]Q.-Y. Tang and Y.-Q. Ma, J. Phys. Chem. B **113**, 10117 (2009).
[66]Q. Zhang, S. Gupta, T. Emrick, and T. P. Russell, J. Am. Chem. Soc. **128**, 3898 (2006).
[67]R. B. Thompson, V. V. Ginzburg, M. W. Matsen, and A. C. Balazs, Science **292**, 2469 (2001).
[68]K. Beneut, D. Constantin, P. Davidson, A. Dessombz, and C. Chaneac, Langmuir **24**, 8205 (2008).
[69]R. D. Deshmukh, Y. Liu, and R. J. Composto, Nano Lett. **12**, 3662 (2007).
[70]A. J. Schultz, C. K. Hall, and J. Genzer, Macromolecules **38**, 3007 (2005).
[71]D. Kechrakos and K. N. Trohidou, Physica B **318**, 360 (2002).

This article is copyrighted as indicated in the article. Reuse of AIP content is subject to the terms at: http://scitation.aip.org/termsconditions. Downloaded to IP: 140.110.200.41 On: Thu, 31 Dec 2015 02:28:59